

Pseudogap-like phase in $\text{Ca}(\text{Fe}_{1-x}\text{Co}_x)_2\text{As}_2$ revealed by ^{75}As NQR

S.-H. Baek,* H.-J. Grafe, L. Harnagea, S. Singh, S. Wurmehl, and B. Büchner
IFW-Dresden, Institute for Solid State Research, PF 270116, 01171 Dresden, Germany
 (Dated: June 21, 2018)

We report ^{75}As NQR measurements on single crystalline $\text{Ca}(\text{Fe}_{1-x}\text{Co}_x)_2\text{As}_2$ ($0 \leq x \leq 0.09$). The nuclear spin-lattice relaxation rate T_1^{-1} as a function of temperature T and Co dopant concentration x reveals a gradual decrease of $(T_1T)^{-1}$ below a crossover temperature T^* in the under- and optimally-doped region. Since there is no hint of a thermodynamic phase transition near T^* , this spin-gap behavior is attributed to the presence of a pseudogap-like novel state of electrons above T_c . The resulting x - T phase diagram shows that, after suppression of the spin-density-wave order, T^* intersects T_c falling to zero rapidly near the optimal doping regime. Possible origins of the pseudogap behavior are discussed.

I. INTRODUCTION

The newly discovered iron-based pnictide superconductors (iron pnictides) show some striking similarities with the cuprates. They are composed of a layered structure with electronically-active planes containing Fe or Cu, respectively. Superconductivity arises from magnetically ordered parents by suppressing the magnetism through chemical doping or pressure.¹ Despite a large effort in recent years, there has been no conclusive answer as to whether the iron pnictides share the same underlying physics with the cuprates. Beyond a probably different superconducting gap symmetry,²⁻⁴ an important difference is that the parent compounds of iron pnictides are itinerant. Electronic correlations are less important and there is no obvious link to Mott physics.⁵⁻⁷ So far, there is no consensus about the precise nature of the normal state in iron pnictides, which is crucial to understand the high temperature superconductivity. A key question is whether there exists an exotic state of matter in the normal state, equivalent to the pseudogap phase in cuprates,^{8,9} and where it originates from.¹⁰⁻¹² In particular, in iron pnictides there are inconsistencies with respect to what can rightfully be called a pseudogap behavior, with contradicting experimental evidence on its presence itself, on its doping dependence, and on the region of the phase diagram where it would occur.¹³⁻¹⁸

While the nuclear spin-lattice relaxation rate T_1^{-1} has proven to be an excellent probe of the pseudo spin-gap phase in most cuprates,^{19,20} it has not been successful in identifying such a novel phase, particularly, in the underdoped region of the iron pnictides. Instead, strong antiferromagnetic (AFM) spin fluctuations (SF) above the magnetic order exist in undoped compounds, and persist even up to optimal doping in the superconducting samples,²¹⁻²⁵ leading to a boost of $(T_1T)^{-1}$ above the magnetic or superconducting transition temperature. Uniquely among iron pnictides, the parent compound CaFe_2As_2 does not show such strong SF above the magnetic and structural transition temperatures $T_N = T_S$.²⁶ Thus, CaFe_2As_2 could be an ideal system to search the pseudogap-like phase which may arise from the weak electron correlations.

In this paper, we present a systematic ^{75}As NQR study of $\text{Ca}(\text{Fe}_{1-x}\text{Co}_x)_2\text{As}_2$ ($0 \leq x \leq 0.09$) focusing on the doping dependent normal state properties. In the under- and optimally-doped regions, measurements of T_1^{-1} show an anomalous suppression in the spectral weight of the low-energy spin dynamics below a crossover temperature T^* , i.e. pseudogap-like behavior. In contrast to other iron pnictides, T^* shows a strong doping-dependence, falling to zero near optimal doping.

II. SAMPLE PREPARATION AND EXPERIMENTAL DETAILS

Single crystals of $\text{Ca}(\text{Fe}_{1-x}\text{Co}_x)_2\text{As}_2$ were grown in Sn flux and their basic physical properties have been well characterized.^{18,27,28} ^{75}As ($I = 3/2$) nuclear quadrupole resonance (NQR) measurements were carried out in 5 different compositions of $\text{Ca}(\text{Fe}_{1-x}\text{Co}_x)_2\text{As}_2$ in the range $0 \leq x \leq 0.09$, where the Co concentration x was determined by energy dispersive x-ray (EDX) analysis. The samples measured in our study are identical to those used in Ref. 28 and therefore we used throughout this paper the SDW transition T_N , the structural transition T_S , and the superconducting transition T_c obtained in Ref. 28. We also confirmed the occurrence of AFM order at T_N from the NQR spectrum which is considerably broadened below $\sim T_N$ due to the distribution of the local field at the nuclear sites, suggesting incommensurate magnetic order.

Often, NQR is advantageous over NMR since it does not require an external field that may induce additional magnetic effects. In fact, the single crystals of $\text{Ca}(\text{Fe}_{1-x}\text{Co}_x)_2\text{As}_2$ are extremely soft so that an external field can cause very inhomogeneous NMR broadening, which strongly varies depending on each piece of crystal, making NMR rather inappropriate to study a systematic doping dependence. The material, however, features a large ^{75}As nuclear quadrupole frequency ν_Q , which allows NQR without the need for an external magnetic field.

T_1^{-1} was obtained by the saturation recovery method, where the relaxation of the nuclear magnetization after a saturating pulse was fitted with a single exponential

function,

$$1 - M(t)/M(\infty) = a \exp(-3t/T_1), \quad (1)$$

where M is the nuclear magnetization and a a fitting parameter that is ideally one. Since the total linewidth of the NQR spectrum is somewhat broader than the bandwidth of the NQR resonant circuit, in particular for larger doping as shown in Fig. 1, we carefully measured T_1^{-1} in order to avoid any artifact such as spectral diffusion. In most cases, however, the data are well fitted using the above function, as shown in Fig. 2 for the optimally doped compound. Also, we confirmed that T_1^{-1} is unique over the whole spectrum.

III. RESULTS AND DISCUSSION

Fig. 1 shows the ^{75}As NQR spectra of $\text{Ca}(\text{Fe}_{1-x}\text{Co}_x)_2\text{As}_2$ for different Co concentrations x at room temperature and their fits to Gaussian lines.²⁹ The linewidth of the spectrum increases with increasing x , as expected from a progressively increasing inhomogeneous distribution of the electric field gradient (EFG). The linewidth of 400 kHz at $x = 0$ increases up to 950 kHz at $x = 0.09$. Interestingly, the resonance frequency, which is the same as ν_Q for $I = 3/2$ in the axial symmetry, slightly increases with increasing x . Similar behavior was also reported in $R\text{FeAs}(\text{O}_{1-x}\text{F}_x)$ ($R=\text{La}, \text{Sm}$).²⁴ The origin of the behavior of $\nu_Q(x)$ is unknown, but the multi-orbital electronic states of Fe^{2+} (d^6) and considerable overlap with p -orbitals of the As ion could be very sensitive to dopants, giving rise to the increase of the EFG at the ^{75}As . A detailed analysis of the EFG and its temperature dependence in $\text{Ca}(\text{Fe}_{1-x}\text{Co}_x)_2\text{As}_2$ will be reported elsewhere.

In Fig. 3 (a) and (b), T_1^{-1} and $(T_1T)^{-1}$, respectively, measured at the peak of the ^{75}As NQR spectra, are shown as a function of temperature and x . Above 200 K, $(T_1T)^{-1}$ is independent of temperature, and insensitive to x for all compositions including the undoped compound. While this is in contrast to other pnictides where $(T_1T)^{-1}$ is reduced with increasing doping, and still shows a temperature dependence, the constant behavior of $(T_1T)^{-1}$ in $\text{Ca}(\text{Fe}_{1-x}\text{Co}_x)_2\text{As}_2$ indicates a weakening of correlations and a convergence to Fermi liquid (FL) behavior at high temperatures. Thus, the unique behavior of $(T_1T)^{-1}$ in $\text{Ca}(\text{Fe}_{1-x}\text{Co}_x)_2\text{As}_2$ among iron pnictides indicates a substantial weakening of AFM SF due to the strongly first order SDW transition whose nature is well preserved against doping. It is also noticeable that $(T_1T)^{-1} = 0.97 \text{ s}^{-1}\text{K}^{-1}$ in $\text{Ca}(\text{Fe}_{1-x}\text{Co}_x)_2\text{As}_2$ is much larger than the values in other iron pnictides e.g., an order of magnitude larger^{21,24} than in 1111 and a factor of three larger even for the isostructural BaFe_2As_2 .^{22,30} The large value $(T_1T)^{-1}$ is ascribed to the larger spectral density of spin fluctuations as compared to other iron pnictides.²⁶ Together with the largest ν_Q among 1111 and 122 materials, it appears that the material is the

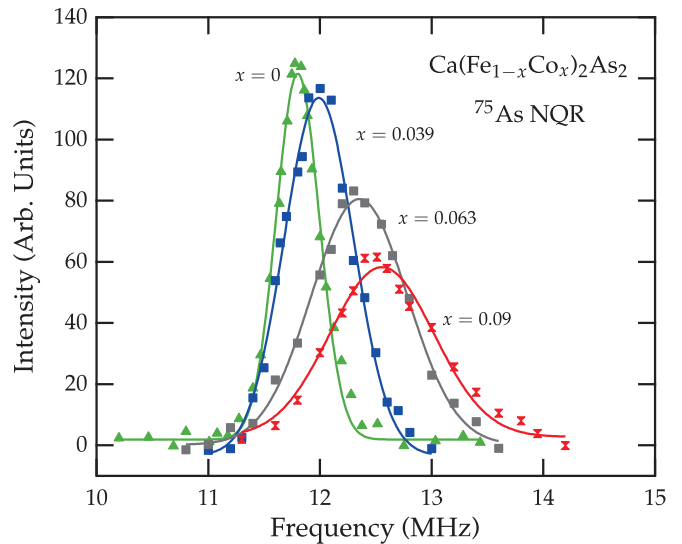


FIG. 1: ^{75}As NQR spectra in $\text{Ca}(\text{Fe}_{1-x}\text{Co}_x)_2\text{As}_2$ ($0 \leq x \leq 0.09$) at room temperature. Both resonance frequency ν_Q and linewidth increase with increasing x .

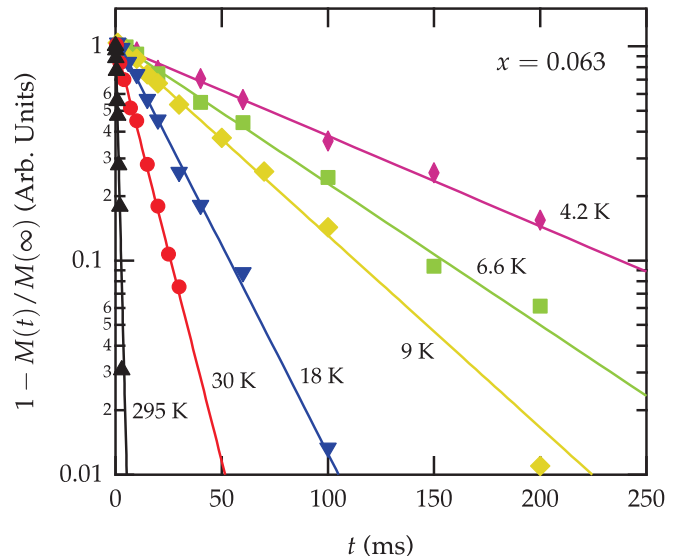


FIG. 2: Recovery of the ^{75}As nuclear magnetization $M(t)$ as a function of time t for optimally doped $\text{Ca}(\text{Fe}_{1-x}\text{Co}_x)_2\text{As}_2$ ($x = 0.063$). Single exponential function (solid lines) fits data quite well in the whole temperature range investigated.

most extreme iron pnictide regarding the sensitivity to the out-of-plane structure.

In the parent compound ($x = 0$), weak but distinct enhancement of $(T_1T)^{-1}$ is visible below 200 K down to T_N . In $\text{Ca}(\text{Fe}_{1-x}\text{Co}_x)_2\text{As}_2$, the EFG at the ^{75}As is directed along the c axis, quantizing nuclei along c . Thus, the relaxation of the ^{75}As on the NQR is expected to be the same as that on the NMR for $H \parallel c$, unless the relaxation mechanism is different for the two cases. Indeed, the $(T_1T)^{-1}$ data measured by NQR are in excellent agreement with previous ^{75}As NMR results²⁶ in

the external field $H \parallel c$, confirming that the weak enhancement of $(T_1T)^{-1}$ above T_N reflects intrinsic low-energy spin dynamics in the material, as well as demonstrating good experimental resolution. At a doping level of $x = 0.039$, $(T_1T)^{-1}$ replicates the data of the parent compound with decreasing temperature. Then, soon after passing $T_N(x = 0)$, an unexpected suppression of $(T_1T)^{-1}$ is observed at a temperature higher than $T_N(x = 0.039)$. Here, the temperature below which $(T_1T)^{-1}$ shows an anomalous suppression is defined as a crossover temperature T^* . With further increasing x to 0.056, T^* is slightly reduced, while T_N is markedly suppressed. At the optimal doping of $x = 0.063$, the SDW is completely suppressed, but the maximum in $(T_1T)^{-1}$ is still clearly visible and T^* is further reduced. The peak of $(T_1T)^{-1}$ centered at T^* broadens with increasing x up to the optimal doping, and disappears in the overdoped region ($x = 0.09$).

Generally, $(T_1T)^{-1}$ can be expressed in terms of the dynamical spin susceptibility $\chi''(\mathbf{q}, \omega_0)$,³¹

$$(T_1T)^{-1} \propto \gamma_n^2 \sum_{\mathbf{q}} A^2(\mathbf{q}) \chi''(\mathbf{q}, \omega_0), \quad (2)$$

where γ_n is the nuclear gyromagnetic ratio, $A(\mathbf{q})$ the \mathbf{q} -dependent hyperfine coupling constant, and $\chi''(\mathbf{q}, \omega_0)$ the imaginary part of the dynamical susceptibility at the Larmor frequency ω_0 . Since A is usually temperature independent, the suppression of $(T_1T)^{-1}$ indicates that the low energy dynamical susceptibility decreases below T^* , exhibiting spin gap-like behavior. Clearly, T^* is well separated from T_N as well as T_c , as shown in Fig. 4.²⁸ We emphasize that T^* is not associated with the structural transition at T_S either. Although T_S seems to be decoupled from T_N with doping,²⁸ T_S occurs slightly above T_N but well below T^* . In our NQR study, however, we could not observe any visible change of the NQR frequency ν_Q or EFG, which is a good probe of the structural transition, near T^* even down to T_N . Furthermore, at optimal doping, both T_N and T_S disappear,²⁸ while T^* is clearly observed (see Fig. 4). Therefore, T^* is interpreted as a crossover temperature below which the pseudogap-like phase emerges.

From these observations, together with T_N and T_c extracted from the uniform magnetic susceptibility measurements,²⁸ we draw the phase diagram of $\text{Ca}(\text{Fe}_{1-x}\text{Co}_x)_2\text{As}_2$ in Fig. 4. T_c is depicted together with the superconducting (SC) volume fraction, which was estimated from the diamagnetic response of the susceptibility in zero field cooled measurements.²⁸ It is noteworthy that “bulk” superconductivity with 100 % SC volume is achieved only in the vicinity of optimal-doping and the SC volume fraction diminishes rapidly with underdoping or overdoping. For example, for $x = 0.039$, only 10 % of the sample volume is estimated to be superconducting. This trend rules out the role of chemical inhomogeneities for the sizable change of the SC volume fraction. Rather, it is likely the result of the competition between the SDW and the SC phase. In support of this,

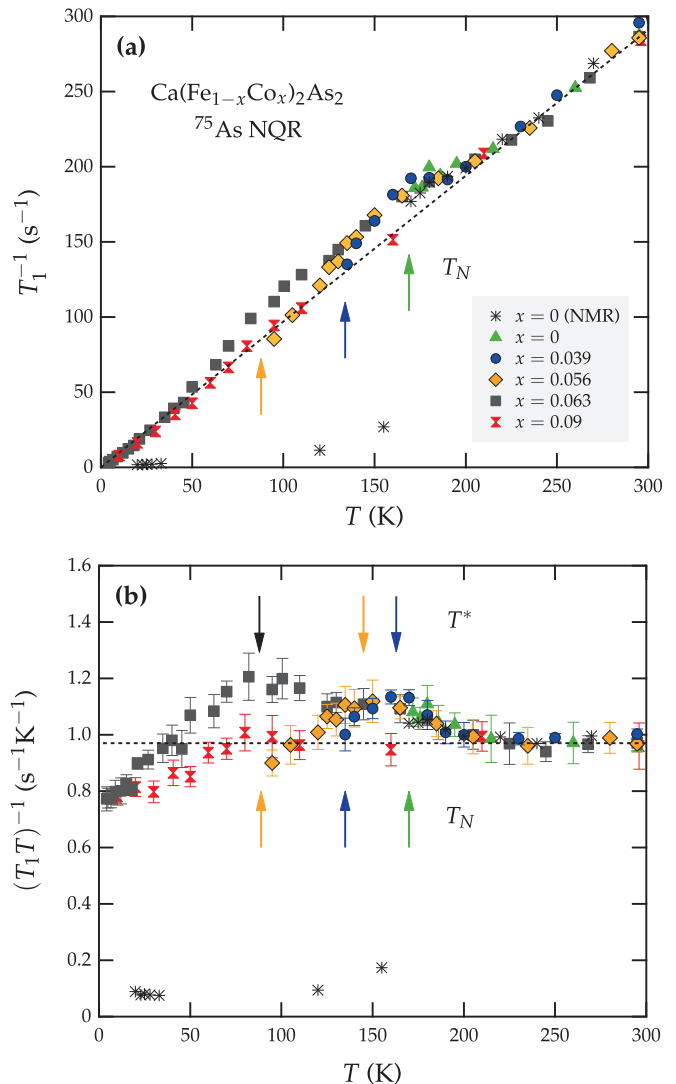


FIG. 3: Nuclear spin-lattice relaxation rate T_1^{-1} versus temperature. Up arrows denote the SDW transition temperature T_N . T_N is not observed at optimal $x = 0.063$ and above.

the SC volume seems to increase linearly as T_N is reduced reaching 100 % immediately after T_N is completely suppressed.

Up to now, pseudogap behavior in other iron pnictides has been inferred from a decrease of the static susceptibility^{18,21,22} (Knight shift and macroscopic susceptibility measured by SQUID) or from a concomitant decrease of $(T_1T)^{-1}$ with decreasing temperature at high temperatures.^{22,32} Even in $\text{Ca}(\text{Fe}_{1-x}\text{Co}_x)_2\text{As}_2$, the static susceptibility shows a similar behavior.¹⁸ However, a doping dependence of such a pseudogap behavior has never been observed, lacking a relationship to superconductivity as well as to the SDW phase at lower doping levels. In contrast, our data reveal the strong doping dependence of T^* in the under- and optimally-doped region as shown in the phase diagram (Fig. 4), which is analogous to that observed in cuprates. Furthermore, we

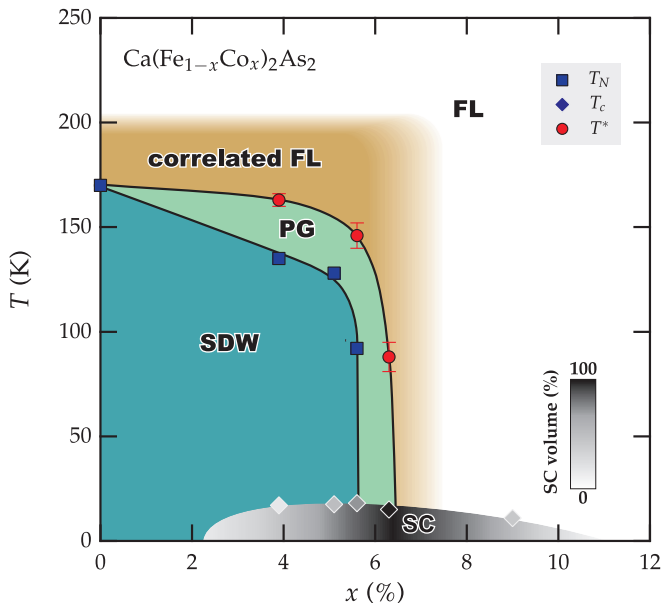


FIG. 4: T - x phase diagram in $\text{Ca}(\text{Fe}_{1-x}\text{Co}_x)_2\text{As}_2$ obtained by $(T_1T)^{-1}$ measurements on the ^{75}As NQR and by the uniform magnetic susceptibility χ_{DC} . FL and PG represent Fermi liquid and pseudogap, respectively. Superconducting volume fraction was estimated by the diamagnetic response of χ_{DC} .

could not observe any anomaly at T_c for optimal doping, which is also similar to underdoped cuprates.²⁰ Nevertheless, the weak temperature dependence of T_1^{-1} in the superconducting state is unexpected, and has only been observed in heavily overdoped $\text{Ba}_{1-x}\text{K}_x\text{Fe}_2\text{As}_2$.³³

Besides, the suggested pseudogap size is unlikely large, being inconsistent with its very weak effect demonstrated in our study. In the isostructural Ba analog $\text{Ba}(\text{Fe}_{1-x}\text{Co}_x)_2\text{As}_2$,^{22,23} for example, a doping independent gap magnitude of $\Delta_{\text{PG}} \gtrsim 450$ K has been estimated from the Knight shift and $(T_1T)^{-1}$, using the phenomenological pseudogap function, $(T_1T)^{-1}$ or $\mathcal{K} \propto \exp(-\Delta_{\text{PG}}/T)$. In comparison, in $\text{Ca}(\text{Fe}_{1-x}\text{Co}_x)_2\text{As}_2$, the similar fit to $(T_1T)^{-1}$ data below T^* for optimal $x = 0.063$ [Fig. 3(b)] gives rise to $\Delta_{\text{PG}} \sim 50$ K, which is an order of magnitude smaller than the values inferred in the Ba-counterpart. Then, the pseudogap behavior in other iron pnictides may be outweighed by AFM correlations that cause an upturn of $(T_1T)^{-1}$. A conservation of the first order character of the SDW transition³⁴ in $\text{Ca}(\text{Fe}_{1-x}\text{Co}_x)_2\text{As}_2$ may inhibit strong AFM correlations, allowing the observation of the pseudogap behavior. Note that also in some cuprates as, for example, $\text{La}_{2-x}\text{Sr}_x\text{CuO}_4$, an upturn of $(T_1T)^{-1}$ is observed instead of a pseudogap, which is presumably due to short-range AFM correlations.

Now we discuss the possible origin of the pseudogap-like phase in $\text{Ca}(\text{Fe}_{1-x}\text{Co}_x)_2\text{As}_2$. In the phase diagram, T^* appears to merge with T_N as $x \rightarrow 0$, and falls steeply to zero intersecting the SC dome near optimal doping (100 % SC volume fraction) where the long range SDW order disappears. $T^* \sim T_N$ at $x = 0$ and the similar

doping dependences of both T^* and T_N suggest that the pseudogap and the SDW may originate from the same physical basis. Also, the existence of T^* at $x = 0$ suggests the itinerant origin of the pseudogap. In comparison, in undoped cuprates i.e., Mott insulators, the pseudogap is always absent. Indeed, a recent NMR study of $\text{Bi}_2\text{Sr}_{2-x}\text{La}_x\text{CuO}_{6+\delta}$ reveals that the pseudogap ground state is metallic and that it is suppressed abruptly near the antiferromagnetic ordered, Mott insulating phase.³⁵ One may speculate that the pseudogap emerges from the *incomplete* nesting of the Fermi surface, which is not associated with the SDW order. Since doping would degrade the nesting condition progressively, both T^* and T_N are decoupled with increasing doping.

From the seeming correlation between T^* and T_c near optimal doping in the phase diagram and from the incomplete nesting scenario as an origin of the pseudogap, one may conjecture an intriguing scenario that the pseudogap is an *incoherent* spin-gapped phase as a precursor state for the coherent SC phase. Recent Andreev reflection studies in $\text{Ba}(\text{Fe}_{1-x}\text{Co}_x)_2\text{As}_2$ reveal phase-incoherent SC pairs³⁶ above T_c which may support this scenario. The weak superconductivity (20% SC volume) in the overdoped region ($x = 0.09$) can be also explained in this scenario since a drop of $(T_1T)^{-1}$ at 60 K [Fig. 3(b)] may indicate the remaining pseudogap that coexists with the dominating FL phase.

IV. CONCLUSION

In conclusion, we have measured the spin lattice relaxation rate, T_1^{-1} , by means of ^{75}As NQR in $\text{Ca}(\text{Fe}_{1-x}\text{Co}_x)_2\text{As}_2$. At high temperatures, $(T_1T)^{-1}$ is independent of doping and temperature. With lowering temperature, $(T_1T)^{-1}$ as a function of x and T reveals a pseudogap behavior.

In contrast to other iron pnictides, the pseudogap in $\text{Ca}(\text{Fe}_{1-x}\text{Co}_x)_2\text{As}_2$ is strongly doping dependent, and appears to be an order of magnitude smaller. From the doping dependence shown in the x - T phase diagram, we interpret that the pseudogap is strongly related to the SDW ordered phase at low doping, and could be a precursor state for the coherent SC phase. Moreover, the T dependence of the static susceptibility (Knight shift) is other than that of the spin lattice relaxation, which puts constraints on theoretical descriptions of the pseudogap behavior in iron pnictides.

Acknowledgment

We thank M. Deuschmann, S. Pichl, and J. Werner for experimental help, and G. Lang for discussion. This work has been supported by the Deutsche Forschungsgemeinschaft through SPP1458 (Grants No. GR3330/2 and No. BE1749/13).

- * sbaek.fu@gmail.com
- ¹ M. D. Lumsden and A. D. Christianson, *J. Phys.: Condens. Matter* **22**, 203203 (2010).
 - ² I. I. Mazin, D. J. Singh, M. D. Johannes, and M. H. Du, *Phys. Rev. Lett.* **101**, 057003 (2008).
 - ³ J. D. Fletcher, A. Serafin, L. Malone, J. G. Analytis, J.-H. Chu, A. S. Erickson, I. R. Fisher, and A. Carrington, *Phys. Rev. Lett.* **102**, 147001 (2009).
 - ⁴ H. Kontani and S. Onari, *Phys. Rev. Lett.* **104**, 157001 (2010).
 - ⁵ A. Koitzsch, D. Inosov, J. Fink, M. Knupfer, H. Eschrig, S. V. Borisenko, G. Behr, A. Köhler, J. Werner, B. Büchner, et al., *Phys. Rev. B* **78**, 180506 (2008).
 - ⁶ T. Kroll, S. Bonhommeau, T. Kachel, H. A. Dürr, J. Werner, G. Behr, A. Koitzsch, R. Hübel, S. Leger, R. Schönfelder, et al., *Phys. Rev. B* **78**, 220502 (2008).
 - ⁷ P. Hansmann, R. Arita, A. Toschi, S. Sakai, G. Sangiovanni, and K. Held, *Phys. Rev. Lett.* **104**, 197002 (2010).
 - ⁸ T. Timusk and B. Statt, *Rep. Prog. Phys.* **62**, 61 (1999).
 - ⁹ M. R. Norman, D. Pines, and C. Kallin, *Adv. Phys.* **54**, 715 (2005).
 - ¹⁰ H. Ikeda, *J. Phys. Soc. Jpn.* **77**, 123707 (2008).
 - ¹¹ H. Lee, Y.-Z. Zhang, H. O. Jeschke, and R. Valentí, *Phys. Rev. B* **81**, 220506 (2010).
 - ¹² H. Ishida and A. Liebsch, *Phys. Rev. B* **81**, 054513 (2010).
 - ¹³ T. Sato, S. Souma, K. Nakayama, K. Terashima, K. Sugawara, T. Takahashi, Y. Kamihara, M. Hirano, and H. Hosono, *J. Phys. Soc. Jpn.* **77**, 063708 (2008).
 - ¹⁴ C. Hess, A. Kondrat, A. Narduzzo, J. E. Hamann-Borrero, R. Klingeler, J. Werner, G. Behr, and B. Büchner, *Europhys. Lett.* **87**, 17005 (2009).
 - ¹⁵ T. Mertelj, V. V. Kabanov, C. Gadermaier, N. D. Zhigadlo, S. Katrych, J. Karpinski, and D. Mihailovic, *Phys. Rev. Lett.* **102**, 117002 (2009).
 - ¹⁶ Y. S. Kwon, J. B. Hong, Y. R. Jang, H. J. Oh, Y. Y. Song, B. H. Min, T. Iizuka, S. Kimura, A. V. Balatsky, and Y. Bang, arXiv:1007.3617 (unpublished).
 - ¹⁷ F. Massee, Y. K. Huang, J. Kaas, E. van Heumen, S. de Jong, R. Huisman, H. Luigjes, J. B. Goedkoop, and M. S. Golden, *Europhys. Lett.* **92**, 57012 (2010).
 - ¹⁸ R. Klingeler, N. Leps, I. Hellmann, A. Popa, U. Stockert, C. Hess, V. Kataev, H.-J. Grafe, F. Hammerath, G. Lang, et al., *Phys. Rev. B* **81**, 024506 (2010).
 - ¹⁹ W. W. Warren, R. E. Walstedt, G. F. Brennert, R. J. Cava, R. Tycko, R. F. Bell, and G. Dabbagh, *Phys. Rev. Lett.* **62**, 1193 (1989).
 - ²⁰ K. Ishida, K. Yoshida, T. Mito, Y. Tokunaga, Y. Kitaoka, K. Asayama, Y. Nakayama, J. Shimoyama, and K. Kishio, *Phys. Rev. B* **58**, R5960 (1998).
 - ²¹ Y. Nakai, K. Ishida, Y. Kamihara, M. Hirano, and H. Hosono, *J. Phys. Soc. Jpn.* **77**, 073701 (2008).
 - ²² F. Ning, K. Ahilan, T. Imai, A. S. Sefat, R. Jin, M. A. McGuire, B. C. Sales, and D. Mandrus, *J. Phys. Soc. Jpn.* **78**, 013711 (2009).
 - ²³ F. L. Ning, K. Ahilan, T. Imai, A. S. Sefat, M. A. McGuire, B. C. Sales, D. Mandrus, P. Cheng, B. Shen, and H.-H. Wen, *Phys. Rev. Lett.* **104**, 037001 (2010).
 - ²⁴ G. Lang, H.-J. Grafe, D. Paar, F. Hammerath, K. Manthey, G. Behr, J. Werner, and B. Büchner, *Phys. Rev. Lett.* **104**, 097001 (2010).
 - ²⁵ A. P. Dioguardi, N. apRoberts Warren, A. C. Shockley, S. L. Bud'ko, N. Ni, P. C. Canfield, and N. J. Curro, *Phys. Rev. B* **82**, 140411 (2010).
 - ²⁶ S.-H. Baek, N. J. Curro, T. Klimczuk, E. D. Bauer, F. Ronning, and J. D. Thompson, *Phys. Rev. B* **79**, 052504 (2009).
 - ²⁷ A. K. Pramanik, L. Harnagea, S. Singh, S. Aswartham, G. Behr, S. Wurmehl, C. Hess, R. Klingeler, and B. Büchner, *Phys. Rev. B* **82**, 014503 (2010).
 - ²⁸ L. Harnagea, S. Singh, G. Friemel, N. Leps, D. Bombor, M. Abdel-Hafiez, A. U. B. Wolter, C. Hess, R. Klingeler, G. Behr, et al., *Phys. Rev. B* **83**, 094523 (2011).
 - ²⁹ For optimal- and overdoped samples, a shoulder appears on the high frequency side of the spectra below ~ 90 K ($x = 0.063$) and below ~ 200 K ($x = 0.09$). For the underdoped sample ($x = 0.039$) such a shoulder does not appear above the structural transition temperature, $T_S \sim 140$ K.²⁸ Since T_1^{-1} at the shoulder for optimal doping is confirmed to be the same as the one at the main peak, we conclude that the shoulder arises from a slightly different environment such as the collapsed tetragonal phase.
 - ³⁰ S.-H. Baek, T. Klimczuk, F. Ronning, E. D. Bauer, J. D. Thompson, and N. J. Curro, *Phys. Rev. B* **78**, 212509 (2008).
 - ³¹ T. Moriya, *J. Phys. Soc. Jpn.* **18**, 516 (1963).
 - ³² H.-J. Grafe, D. Paar, G. Lang, N. J. Curro, G. Behr, J. Werner, J. Hamann-Borrero, C. Hess, N. Leps, R. Klingeler, et al., *Phys. Rev. Lett.* **101**, 047003 (2008).
 - ³³ S. W. Zhang, L. Ma, Y. D. Hou, J. Zhang, T.-L. Xia, G. F. Chen, J. P. Hu, G. M. Luke, and W. Yu, *Phys. Rev. B* **81**, 012503 (2010).
 - ³⁴ A. Cano, M. Civelli, I. Eremin, and I. Paul, *Phys. Rev. B* **82**, 020408 (2010).
 - ³⁵ S. Kawasaki, C. Lin, P. L. Kuhns, A. P. Reyes, and G.-q. Zheng, *Phys. Rev. Lett.* **105**, 137002 (2010).
 - ³⁶ G. Sheet, M. Mehta, D. A. Dikin, S. Lee, C. W. Bark, J. Jiang, J. D. Weiss, E. E. Hellstrom, M. S. Rzchowski, C. B. Eom, et al., *Phys. Rev. Lett.* **105**, 167003 (2010).